Human Molecular Genetics, 2012, Vol. 21, No. 14 **3128–3142**
doi:10.1093/hmg/dds140
Advance Access published on April 14, 2012

The GTPase ARFRP1 controls the lipidation of chylomicrons in the Golgi of the intestinal epithelium

Alexander Jaschke[1,†], Bomee Chung[1,†], Deike Hesse[1], Reinhart Kluge[1], Claudia Zahn[1], Markus Moser[2], Klaus-Jürgen Petzke[3], Regina Brigelius-Flohé[4], Dmytro Puchkov[5], Hermann Koepsell[6], Joerg Heeren[7], Hans-Georg Joost[8] and Annette Schürmann[1,*]

[1]Department of Experimental Diabetology, German Institute of Human Nutrition Potsdam-Rehbruecke, D-14558 Nuthetal, Germany, [2]Department of Molecular Medicine, Max Planck Institute of Biochemistry, D-82152 Martinsried, Germany, [3]Section Energy Metabolism, German Institute of Human Nutrition Potsdam-Rehbruecke, D-14558 Nuthetal, Germany, [4]Department of Biochemistry and Micronutrients, German Institute of Human Nutrition Potsdam-Rehbruecke, D-14558 Nuthetal, Germany, [5]Institute of Chemistry and Biochemistry, Freie Universität Berlin, D-14195 Berlin, Germany, [6]Institute of Anatomy and Cell Biology, University of Würzburg, D-97070 Würzburg, Germany, [7]Institute of Biochemistry and Molecular Biology II: Molecular Cell Biology, University Medical Center Hamburg-Eppendorf, D-20246 Hamburg, Germany and [8]Department of Pharmacology, German Institute of Human Nutrition Potsdam-Rehbruecke, D-14558 Nuthetal, Germany

Received December 21, 2011; Revised and Accepted April 4, 2012

The uptake and processing of dietary lipids by the small intestine is a multistep process that involves several steps including vesicular and protein transport. The GTPase ADP-ribosylation factor-related protein 1 (ARFRP1) controls the ARF-like 1 (ARL1)-mediated Golgi recruitment of GRIP domain proteins which in turn bind several Rab-GTPases. Here, we describe the essential role of ARFRP1 and its interaction with Rab2 in the assembly and lipidation of chylomicrons in the intestinal epithelium. Mice lacking *Arfrp1* specifically in the intestine (*Arfrp1*$^{vil-/-}$) exhibit an early post-natal growth retardation with reduced plasma triacylglycerol and free fatty acid concentrations. *Arfrp1*$^{vil-/-}$ enterocytes as well as *Arfrp1* mRNA depleted Caco-2 cells absorbed fatty acids normally but secreted chylomicrons with a markedly reduced triacylglycerol content. In addition, the release of apolipoprotein A-I (ApoA-I) was dramatically decreased, and ApoA-I accumulated in the *Arfrp1*$^{vil-/-}$ epithelium, where it predominantly co-localized with Rab2. The release of chylomicrons from Caco-2 was markedly reduced after the suppression of Rab2, ARL1 and Golgin-245. Thus, the GTPase ARFRP1 and its downstream proteins are required for the lipidation of chylomicrons and the assembly of ApoA-I to these particles in the Golgi of intestinal epithelial cells.

INTRODUCTION

The adequate absorption of lipids is essential for all mammalian species because of their inability to synthesize essential fatty acids and fat-soluble vitamins. The lipid absorption requires several events such as hydrolysis, uptake into the enterocytes, re-esterification and transport into the lymph or portal blood (1–3). About 95% of the lipids in the diet are composed of triacylglycerols which are cleaved via lipolysis to produce free fatty acids and 2-monoacylglycerol. Absorbed

*To whom correspondence should be addressed at: Department of Experimental Diabetology, German Institute of Human Nutrition Potsdam-Rehbruecke, Arthur-Scheunert-Allee 114-116, D-14558 Nuthetal, Germany. Tel: +49-33200882368; Fax: +49-33200882334; Email: schuermann@dife.de
†Both authors contributed equally to this work.

fatty acids and monoacylglycerols are bound to intracellular proteins (fatty acid transport proteins, FATP's) and/or rapidly converted to triacylglycerols to prevent cellular membrane disruption. The triacylglycerol produced at the level of the endoplasmic reticulum (ER) is either incorporated into pre-chylomicrons within the ER lumen or shunted to triacylglycerol storage pools. The pre-chylomicrons exit the ER in a specialized transport vesicle, the PCTV (pre-chylomicron transport vesicle), which is the rate-limiting step in the intracellular transit of triacylglycerol across the enterocyte. The pre-chylomicrons are further processed in the Golgi and transported to the basolateral membrane via a separate vesicular system for exocytosis into the intestinal lamina propria (2,3). Little is known about post-ER maturation and secretion process of chylomicrons in the Golgi.

Here, we describe the essential role of a small *trans*-Golgi-associated GTPase for the maturation and lipidation of chylomicrons. ARFRP1 (ADP-ribosylation factor-related protein 1) is a member of the family of ARFs of GTPases which play a pivotal role in the regulation of membrane traffic (4–6). Activated, GTP-bound ARFRP1 associates with *trans*-Golgi membranes (7,8) and is required for the recruitment of ARF-like 1 (ARL1) and its effector Golgin-245 to the *trans*-Golgi (7,9,10). ARFRP1 is essential for the normal growth of lipid droplets by mediating the transfer of newly formed small lipid particles to the large storage droplets because mice lacking *Arfrp1* specifically in adipocytes ($Arfrp1^{ad-/-}$) were lipodystrophic and exhibited a defective lipid droplet formation in adipose tissues (11).

In order to define the role of ARFRP1 in intestinal nutrient absorption, we characterized intestine-specific *Arfrp1* null mutants ($Arfrp1^{vil-/-}$ mice) with regard to the lipid metabolism. As a consequence of the defective lipidation and maturation of chylomicrons in the Golgi, the triacylglycerol concentration in the plasma of $Arfrp1^{vil-/-}$ mice was markedly reduced resulting in growth retardation.

RESULTS

Growth retardation and lethality of $Arfrp1^{vil-/-}$ mice

Mice lacking intestinal *Arfrp1* ($Arfrp1^{vil-/-}$) were born with no apparent differences in size. Subsequently, poor growth (Fig. 1A) and lethality (Fig. 2A) became evident at the age of 3 days. Measurement of body composition indicated that both fat mass and lean mass of $Arfrp1^{vil-/-}$ mice were reduced (Fig. 1B) resulting in no alteration of the relative body composition. In addition, the weights of the liver and kidney and the length of the small intestine were significantly reduced in $Arfrp1^{vil-/-}$ mice (Supplementary Material, Table S3). However, normalized for the reduced body weight and length of $Arfrp1^{vil-/-}$ mice, the relative intestinal length did not differ ($Arfrp1^{flox/flox}$: 3.74 ± 0.19 vs. $Arfrp1^{vil-/-}$: 3.60 ± 0.20). In parallel with the marked growth retardation, we detected significantly lower levels of glucose, triacylglycerol, free fatty acids and cholesterol in the plasma of $Arfrp1^{vil-/-}$ mice (Supplementary Material, Table S4), whereas plasma concentrations of insulin were not altered ($Arfrp1^{flox/flox}$: 0.299 ± 0.047 vs. $Arfrp1^{vil-/-}$: 0.279 ± 0.029 μg/l). In order to test whether these blood parameters differ due to altered liver function, we studied the expression of mRNA of enzymes involved in glucose and lipid metabolism. Since we did not detect differences, for example, in the mRNA level of the gluconeogenic enzyme PEPCK (*Pck1*) and lipid metabolism (*Acaca*, *Fasn*, *Scd1*, *Cpt1a*, *Hadhsc*; Supplementary Material, Fig. S1), we conclude that $Arfrp1^{vil-/-}$ mice suffer from the lack of nutrients potentially due to malabsorption.

We tried to reduce the lethality of $Arfrp1^{vil-/-}$ mice by a dietary intervention and tested their survival rate under different diets, a standard chow diet (10% fat, 70% carbohydrates and 20% protein; percent of calories), a fat-depleted diet (0.2% fat, 73.2% carbohydrates and 26.5% protein) and a carbohydrate-free fat-enriched diet (72% fat and 28% protein). Under fat-depleted and standard diet conditions, the survival of $Arfrp1^{vil-/-}$ mice (41 and 51% after 35 days, respectively) was much better than under the fat-enriched diet (14%, Fig. 2A). These data suggested that *Arfrp1* is required for an adequate absorption of fat in the small intestine.

Reduced fat absorption of $Arfrp1^{vil-/-}$ mice

Oral fat tolerance tests performed with 5-week-old mice indicated an impaired fat absorption in $Arfrp1^{vil-/-}$ mice: in contrast to controls ($Arfrp1^{flox/flox}$), $Arfrp1^{vil-/-}$ mice failed to respond to a bolus of olive oil by an increase in plasma triacylglycerol (Fig. 2B). Furthermore, the concentration of all fatty acids, including essential and conditionally essential fatty acids (linoleic acid, linolenic acid and γ-linolenic acid), were significantly lower in the plasma of $Arfrp1^{vil-/-}$ than in $Arfrp1^{flox/flox}$ littermates (Supplementary Material, Fig. S2A). Since defective intestinal fat absorption is associated with deficiency in fat-soluble vitamins, we measured vitamin E levels in the plasma and detected significantly lower levels in $Arfrp1^{vil-/-}$ than in control mice (Supplementary Material, Fig. S2B).

During oral glucose tolerance tests, blood glucose concentrations were essentially identical in both genotypes, indicating that glucose transport is not impaired in the absence of *Arfrp1* (Supplementary Material, Fig. S3A). Furthermore, immunohistochemistry demonstrated that SGLT1 was exclusively located at the apical membrane with no differences between control and $Arfrp1^{vil-/-}$ mice (Supplementary Material, Fig. S3B). Western blot analysis confirmed that the expression of glucose transporters SGLT1 and GLUT2 is not impaired in $Arfrp1^{vil-/-}$ mice (Supplementary Material, Fig. S3C).

Levels of most essential and non-essential proteinogenic as well as of non-proteinogenic amino acids were identical in the plasma of $Arfrp1^{flox/flox}$ and $Arfrp1^{vil-/-}$ mice. Concentrations of some amino acids like glycine, glutamine and glutamate were higher in $Arfrp1^{vil-/-}$ than in control mice. Thus, the absorption of peptides and amino acids does not appear to be impaired in the null mutants (Supplementary Material, Fig. S3D).

Since the results described suggested that the growth retardation of $Arfrp1^{vil-/-}$ mice is due to the specific impairment of lipid absorption, we performed quantitative RT–PCR analysis of several transcripts involved in fatty acid transport but failed to detect differences in the expression of the fatty acid

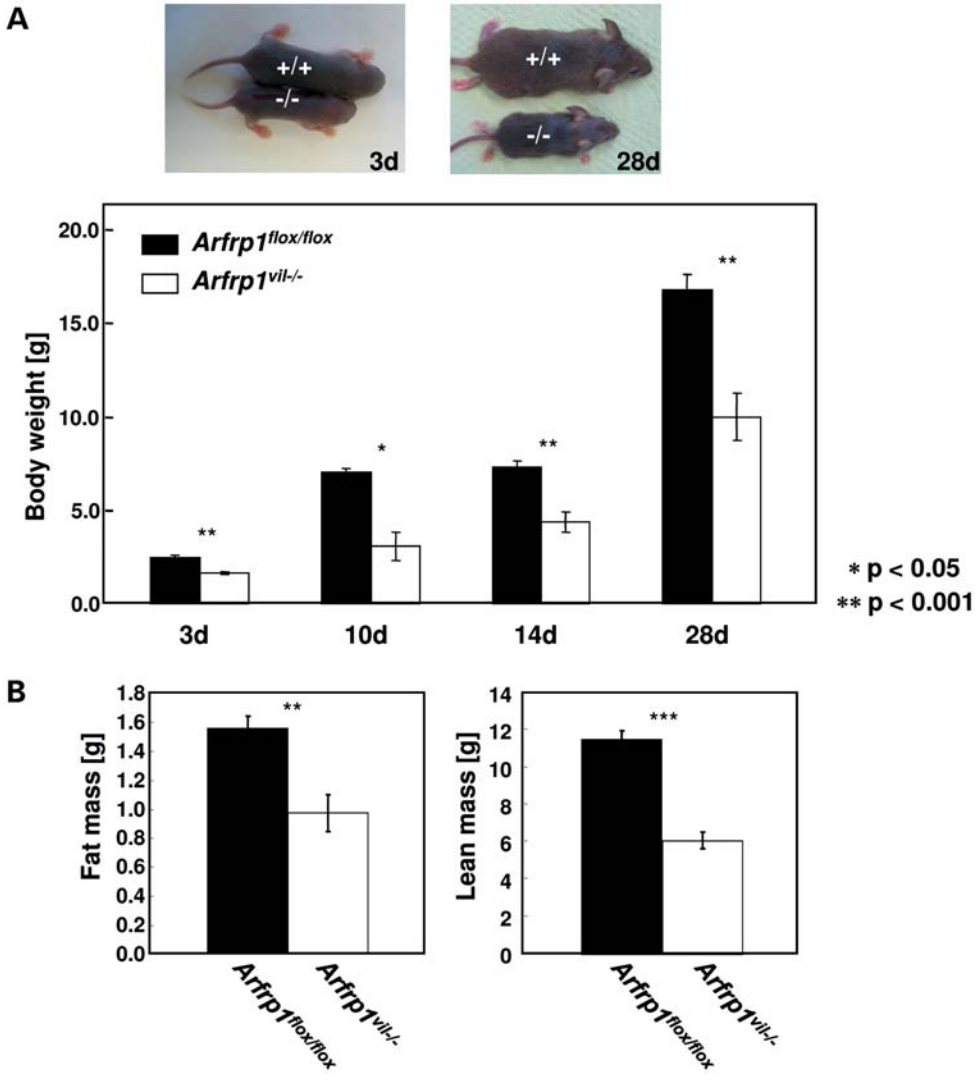

Figure 1. Growth retardation of $Arfrp1^{vil-/-}$ mice. (**A**) Photographs of 3- and 28-day-old $Arfrp1^{flox/flox}$ (+/+) and $Arfrp1^{vil-/-}$ (−/−) mice. Body weights of $Arfrp1^{flox/flox}$ and $Arfrp1^{vil-/-}$ mice at the age of 3–28 days ($n = 10–12$). (**B**) Fat mass (left panel) and lean mass (right panel) of $Arfrp1^{flox/flox}$ ($n = 26$) and $Arfrp1^{vil-/-}$ mice ($n = 10$) at the age of 28 days. Values are means of 10–26 mice ± SEM (**$P < 0.01$, ***$P < 0.001$).

transporters FATP1, FATP4 and CD36 or the fatty acid binding proteins FABP1 and FABP2. Transcripts of enzymes involved in triacylglycerol synthesis (DGAT1 and DGAT2), or those involved in chylomiron production such as ApoB, ApoA-I and microsomal triacylglycerol transfer protein (MTP), were not different between the genotypes (Supplementary Material, Fig. S4A). In addition, no differences in the subcellular localization of FATP1, FABP1 and DGAT2 were detected in the intestinal sections of $Arfrp1^{flox/flox}$ and $Arfrp1^{vil-/-}$ mice (Supplementary Material, Fig. S4B).

In order to test whether fatty acid uptake is affected in the $Arfrp1^{vil-/-}$ epithelium, we stained lipids in sections of jejunum of $Arfrp1^{flox/flox}$ and $Arfrp1^{vil-/-}$ mice with oil red-O 2 h after mice received an oral gavage of olive oil. We did not detect differences; both genotypes accumulated lipid droplets in the intestinal epithelium (Supplementary Material, Fig. S4C, left panels). This finding was confirmed by staining the lipid droplet coat protein TIP47 which also showed a similar distribution in control and $Arfrp1^{vil-/-}$ cells (Supplementary Material, Fig. S4C, right panels). These results indicate that neither the uptake of dietary fat into the intestinal epithelium nor the lipid droplet formation was affected in the absence of ARFRP1.

To test the impact of ARFRP1 on fat absorption in a system of isolated cells, *Arfrp1* expression was suppressed in the colon carcinoma cell line Caco-2 by specific siRNA (Fig. 2C, upper panel), cells incubated with ^{14}C-labeled palmitate for 24 h and the uptake, retention and basolateral release of radioactivity were detected. The fatty acid uptake was not significantly different in Caco-2 cells transfected with scrambled or *Arfrp1*-specific siRNA. However, the retention of radioactivity was slightly but significantly increased after the down-regulation of *Arfrp1*, whereas the release on the basolateral site was markedly reduced in si*Arfrp1* transfected cells (Fig. 2C, lower panels), suggesting that the basolateral export of lipids is affected after the disruption of *Arfrp1*.

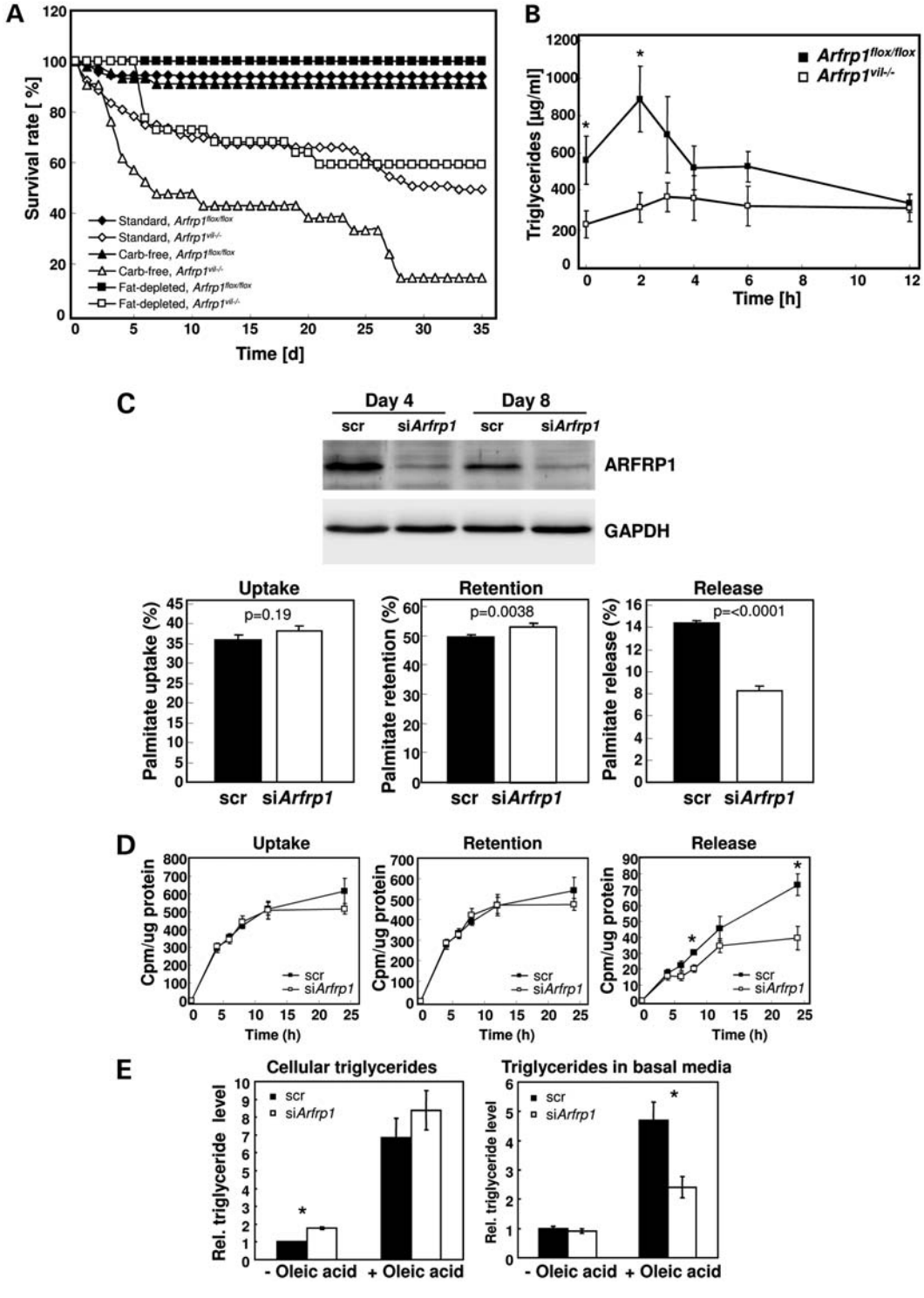

Figure 2. Lethality and impaired triacylglycerol absorption of *Arfrp1*$^{vil-/-}$ mice. (**A**) Survival curves of *Arfrp1*$^{flox/flox}$ and *Arfrp1*$^{vil-/-}$ mice that were fed with either a standard diet, fat-depleted or carbohydrate-free (carb-free) diet over a time period of 35 days. (**B**) Triacylglycerol concentrations during fat tolerance tests performed in 5-week-old *Arfrp1*$^{flox/flox}$ and *Arfrp1*$^{vil-/-}$ mice. Values are means of eight mice ± SEM ($^{*}P < 0.05$). (**C**) Impaired lipid release of Caco-2 cells after the down-regulation of *Arfrp1* expression. Caco-2 cells were transfected with scrambled or *Arfrp1*-specific siRNA and harvested 4 and 8 days after transfection for western blot analysis with the anti-ARFRP1 antiserum (upper panel). Caco-2 cells were incubated with ^{14}C-labeled palmitate for 24 h, and radioactivity was determined in the basolateral medium reflecting the release (lower right panel) and in the lysates of the cells which indicates the retention (lower middle panel). The uptake was calculated as the sum of radioactivity in the cell lysates and the basolateral medium (lower left panel). (**D**) Time course of impaired lipid release from *Arfrp1* knockdown Caco-2 cells. Cells were treated with ^{14}C-labeled palmitate in the apical medium, and lipid transport was measured at the indicated time points over the next 24 h. (**E**) Caco-2 cells transfected with scrambled or *Arfrp1* siRNA were treated with 4 mM oleic acid for 24 h, and triacylglycerol levels in the cells (left panel) and the basal media (right panel) were measured. Values represent the mean ± SEM from three independent experiments ($^{*}P < 0.05$).

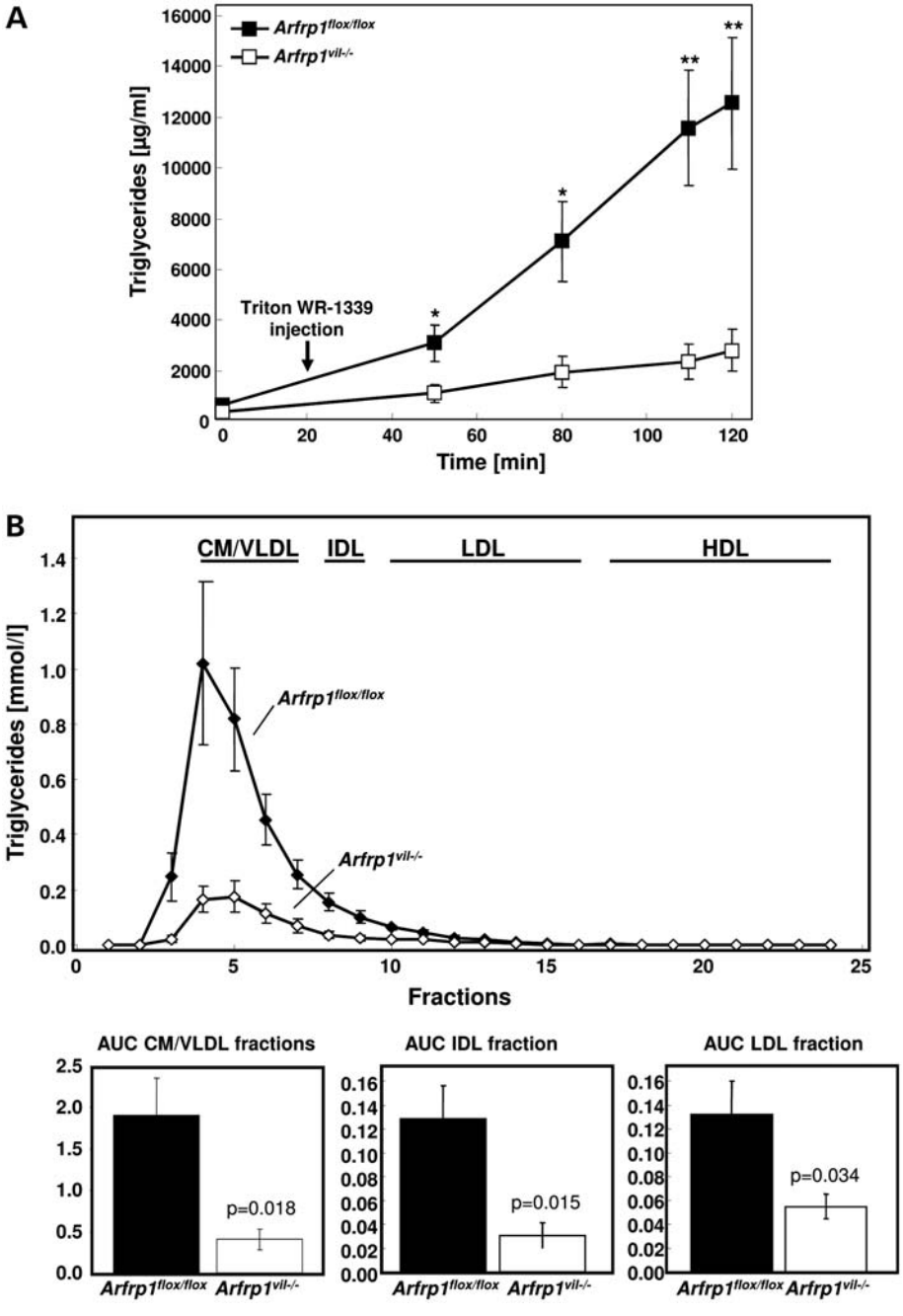

Figure 3. Reduced fat absorption of *Arfrp1*$^{vil-/-}$ mice. (**A**) A fat tolerance test was performed in 5 h fasted *Arfrp1*$^{flox/flox}$ and *Arfrp1*$^{vil-/-}$ mice, and plasma triacylglycerol concentrations were detected at the indicated time points after the inhibition of lipoprotein catabolism by i.v. injection of Triton WR-1339. (**B**) FPLC profiles of plasma samples of *Arfrp1*$^{flox/flox}$ and *Arfrp1*$^{vil-/-}$ mice ($n = 6$) that received an oil bolus plus Triton WR-1339. Triacylglycerol concentrations (mmol/l) were detected in the different fractions, chylomicron/VLDL (fractions 4–7), IDL (fractions 8,9), LDL (fractions 10–16) and HDL (fractions 17–24).

The time course of lipid absorption indicated that the release was reduced early between 6 and 8 h after the addition of radioactive palmitate to si*Arfrp*-transfected cells (Fig. 2D). Similar effects were observed when triacylglycerol levels were measured in Caco-2 cells and in the basal medium before and after incubation with oleic acid (Fig. 2E), suggesting that re-esterified triacylglycerol within the epithelial cells is not adequately released in the absence of *Arfrp1*.

Impaired chylomicron maturation in the Golgi of the *Arfrp1*$^{vil-/-}$ intestinal epithelium

We next performed a fat tolerance test in the presence of Triton WR-1339 which inhibits lipoprotein catabolism. Triacylglycerol concentrations increased constantly over a time period of 2 h in *Arfrp1*$^{flox/flox}$ mice, whereas the triacylglycerol concentrations of *Arfrp1*$^{vil-/-}$ mice were markedly lower

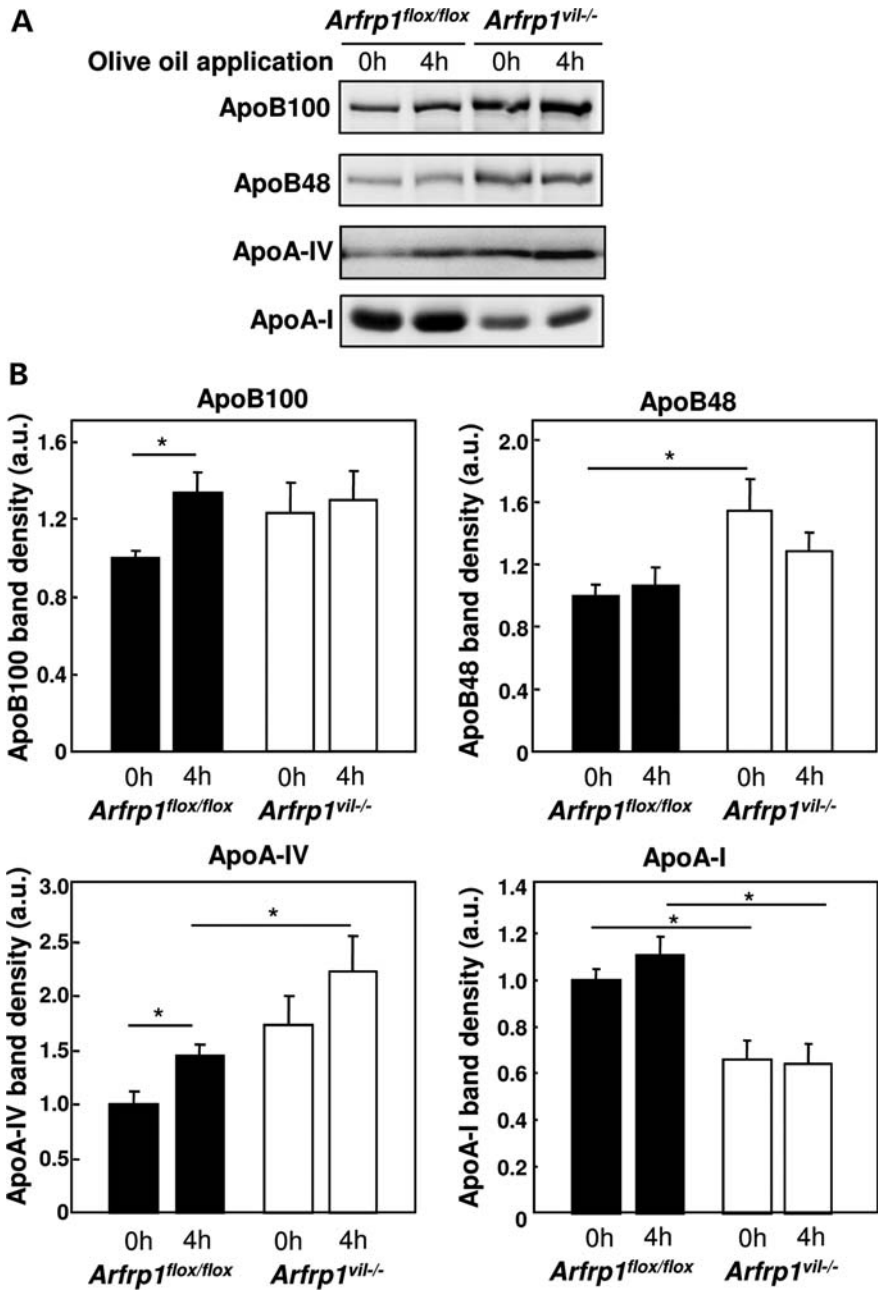

Figure 4. Impaired assembly of ApoA-I to chylomicrons in the intestinal epithelium of *Arfrp1*$^{vil-/-}$ mice. (**A**) Plasma of 16 h fasted *Arfrp1*$^{flox/flox}$ and *Arfrp1*$^{vil-/-}$ mice (0 h) or of mice 4 h after receiving an oil bolus was analyzed by western blotting with the indicated antibodies. (**B**) Quantification of the levels of indicated Apo in the plasma of fasted and oil-treated *Arfrp1*$^{flox/flox}$ and *Arfrp1*$^{vil-/-}$ mice ($n = 10–11$). (**C**) Triacylglycerol concentrations and levels of the indicated Apo in the chylomicron fractions of plasma from *Arfrp1*$^{flox/flox}$ and *Arfrp1*$^{vil-/-}$ mice that had received an oil bolus plus Triton WR-1339. (**D**) Immunohistochemical detection of indicated Apo in the intestinal section of *Arfrp1*$^{flox/flox}$ and *Arfrp1*$^{vil-/-}$ mice that were fasted and sacrificed 2 h after the olive oil bolus. Controls had free access to their regular standard diet. (**E**) Ultrastructural analysis of epithelial cells of *Arfrp1*$^{flox/flox}$ and *Arfrp1*$^{vil-/-}$ mice. Pictures show representative Golgi structures of control and knockout epithelial cells. The arrows depict premature chylomicrons that were rarely visible in the Golgi lumen of control cells but accumulated in that of *Arfrp1*$^{vil-/-}$ cells (G: Golgi apparatus; N: nucleus; CM: chylomicrons).

indicating lower lipid release by chylomicrons in *Arfrp1*$^{vil-/-}$ mice (Fig. 3A). Strikingly, the plasma collected from *Arfrp1*$^{vil-/-}$ mice 2 h after the oil bolus appeared to be transparent and bright, while plasma from *Arfrp1*$^{flox/flox}$ mice was pale and turbid (data not shown). In contrast, Triton WR-1339 injection without the oil bolus did not induce differences in the plasma triacylglycerol concentrations between control and *Arfrp1*$^{vil-/-}$ mice (Supplementary Material, Fig. S5), indicating that hepatic VLDL release is not affected in *Arfrp1*$^{vil-/-}$ mice.

Fractionation of lipids into chylomicrons, IDL, LDL and HDL by FPLC revealed a predominant reduction in triacylglycerol concentrations in the chylomicron/VLDL fraction of *Arfrp1*$^{vil-/-}$ mice (Fig. 3B).

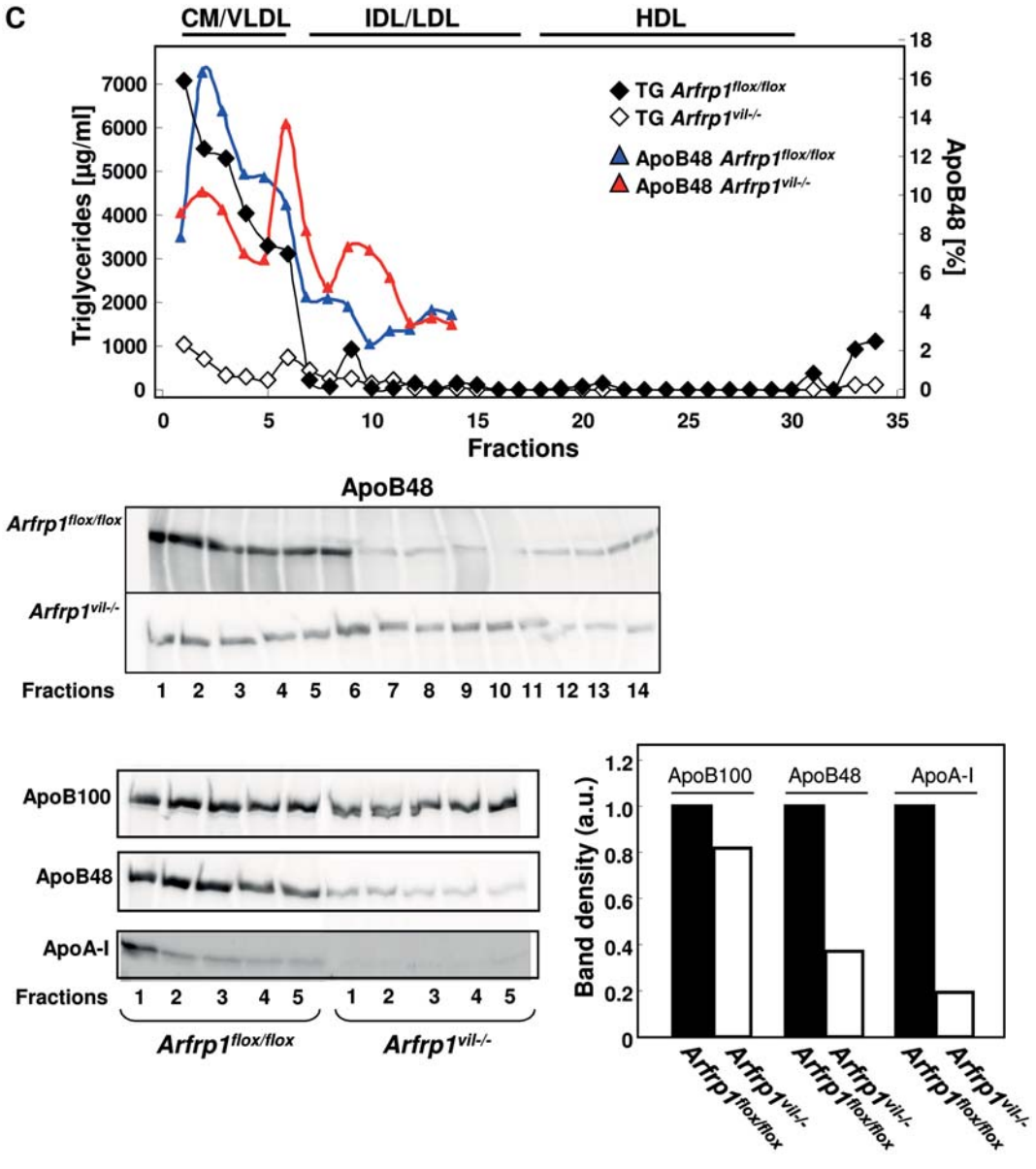

Figure 4. *Continued*

After fatty acids have been converted to triacylglycerol, they are packaged with apolipoproteins (Apo; B48, A-I and A-IV) forming either chylomicrons or very-low-density lipoproteins (VLDLs) (3,12). We determined their levels in the plasma of control and *Arfrp1*$^{vil-/-}$ mice after fasting and 4 h after an olive oil bolus (Fig. 4A and B). The ApoB100 level in the plasma of control mice significantly increased after the lipid application, whereas no changes were detectable in the plasma of *Arfrp1*$^{vil-/-}$ mice. ApoB48 did not change in response to the oil bolus; however, it was significantly higher in the null mutants. ApoA-IV increased when control mice received the oil. *Arfrp1*$^{vil-/-}$ mice showed a similar trend and the ApoA-IV level was constantly higher than in control mice. ApoA-I exhibited the most striking difference with markedly lower plasma concentrations in mice lacking intestinal *Arfrp1* (Fig. 4A and B).

We next studied the levels of Apo in the chylomicron, IDL/LDL and HDL fractions obtained from the plasma of control and *Arfrp1*$^{vil-/-}$ mice that received an oil bolus in combination with Triton WR-1339 after the 5-h fasting period. We confirmed the reduction in triacylglycerol levels in the chylomicron fraction (fractions 1–5) of *Arfrp1*$^{vil-/-}$ mice by ~85% (Fig. 4C) and obtained a similar reduction in cholesterol concentration (Supplementary Material, Fig. S6). The quantification of the ApoB48 levels in the different fractions indicated that they were also reduced in the chylomicron fraction of *Arfrp1*$^{vil-/-}$ mice, but higher in denser fractions (IDL/LDL), indicating that *Arfrp1*$^{vil-/-}$ mice secrete smaller chylomicrons containing less triacylglycerol than control mice (Fig. 4C). In addition, the ApoA-I levels in the chylomiron fractions of *Arfrp1*$^{vil-/-}$ mice were much lower than in the corresponding fractions of control plasma. Thus, enterocytes

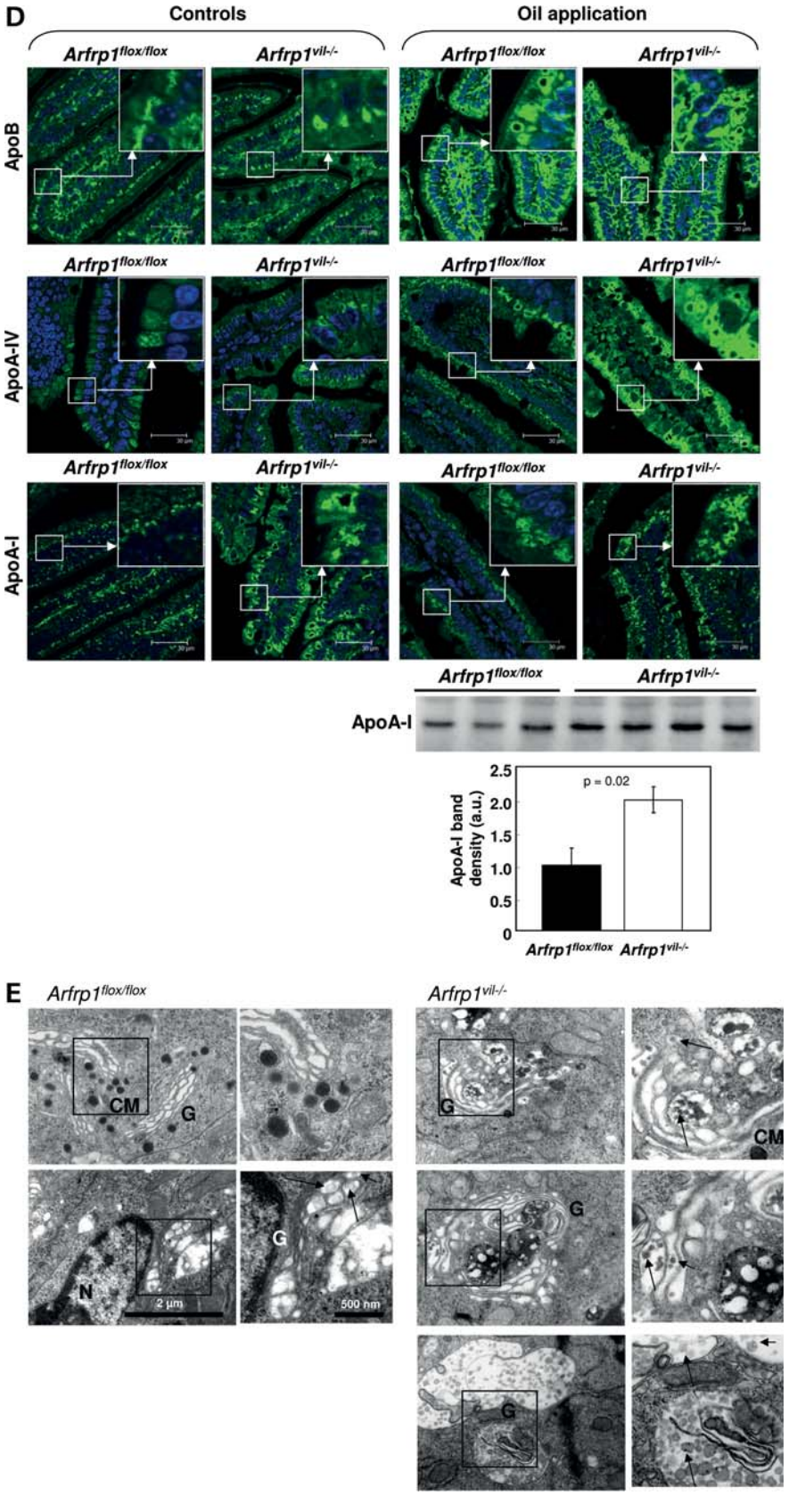

Figure 4. *Continued*

release chylomicrons in the absence of *Arfrp1*, but the lipoprotein–triacylglycerol composition of chylomicrons differs markedly between control and *Arfrp1*$^{vil-/-}$ mice.

Immunostaining of the Apo revealed ApoB generation in both *Arfrp1*$^{flox/flox}$ and *Arfrp1*$^{vil-/-}$ mice by the oil application. However, it showed a dramatic accumulation of ApoA-IV and ApoA-I in the intestinal epithelium of *Arfrp1*$^{vil-/-}$ mice (Fig. 4D). This effect was confirmed by western blotting (Fig. 4D, lower panels) displaying a significant increase in ApoA-I in the intestinal epithelial cells. Ultrastructural analysis of epithelial cells showed a different structure of the Golgi and an accumulation of premature chylomicrons (arrows in Fig. 4E) within the Golgi apparatus in the *Arfrp1*$^{vil-/-}$ epithelial cell. In some knockout cells, we detected bloated vesicles in the area of the Golgi which were enriched with small particles that appear to be premature chylomicrons (lower right panels). Furthermore, we observed a lower number of mature chylomicrons released from the Golgi apparatus of *Arfrp1*$^{vil-/-}$ cells than detected in control cells (Fig. 4E).

We next suppressed *Arfrp1* expression in Caco-2 cells and determined the basolateral release of the Apo by western blotting. As demonstrated in Figure 5A and B, the secretion of ApoB100, ApoB48 and ApoA-IV increased when control cells were treated with oleic acid. Interestingly, the concentration of ApoB100, ApoB48 and ApoA-IV in the basal medium was higher when *Arfrp1* expression was suppressed, whereas that of ApoA-I—like in *Arfrp1*$^{vil-/-}$ mice—was significantly reduced (Fig. 5A and B). Since the effect on reduced ApoA-I release after the suppression of *Arfrp1* expression was smaller than detected in *Arfrp1*$^{vil-/-}$ mice, we compared the *Arfrp1* expression with the levels of ApoA-I in the basal medium. As shown in Supplementary Material, Figure S7, both parameters show a strong correlation ($R^2 = 0.6639$), indicating that the effect of reduced ApoA-I secretion is higher when expression of *Arfrp1* is lower. These data indicate a specific defect in composing chylomicrons in *Arfrp1* knockdown cells which leads to reduced ApoA-I and higher levels of ApoB48 and ApoA-IV and to a reduced capacity to carry triacylglycerol.

Since MTP transfers lipids to the lipoproteins, we tested MTP expression and/or activity. The down-regulation of *Arfrp1* resulted in a rather moderate increase in MTP protein levels and a slight increase in MTP activity, when cells were treated in the absence of oleic acid, whereas no effects were detectable in the presence of oleic acid (Supplementary Material, Fig. S8A). We furthermore stained intestinal sections for MTP but did not observe differences in its subcellular distribution (Supplementary Material, Fig. S8B).

In order to test whether the assembly of ApoA-I to the chylomicron is required for their final lipidation and maturation, we suppressed *ApoA-I* expression in Caco-2 cells and measured cellular triacylglycerol content and triacylglycerol levels in the basal media before and after oleic acid treatment. Here, we did not observe any differences (Fig. 5C), indicating that the assembly of ApoA-I is not involved in the final lipid load to the chylomicrons.

Rab2 co-localizes with ApoA-I and accumulates at the Golgi in the *Arfrp1*$^{vil-/-}$ intestinal epithelium

ARFRP1 is required for the recruitment of ARL1 and its effector, the GRIP domain protein Golgin-245, to *trans*-Golgi

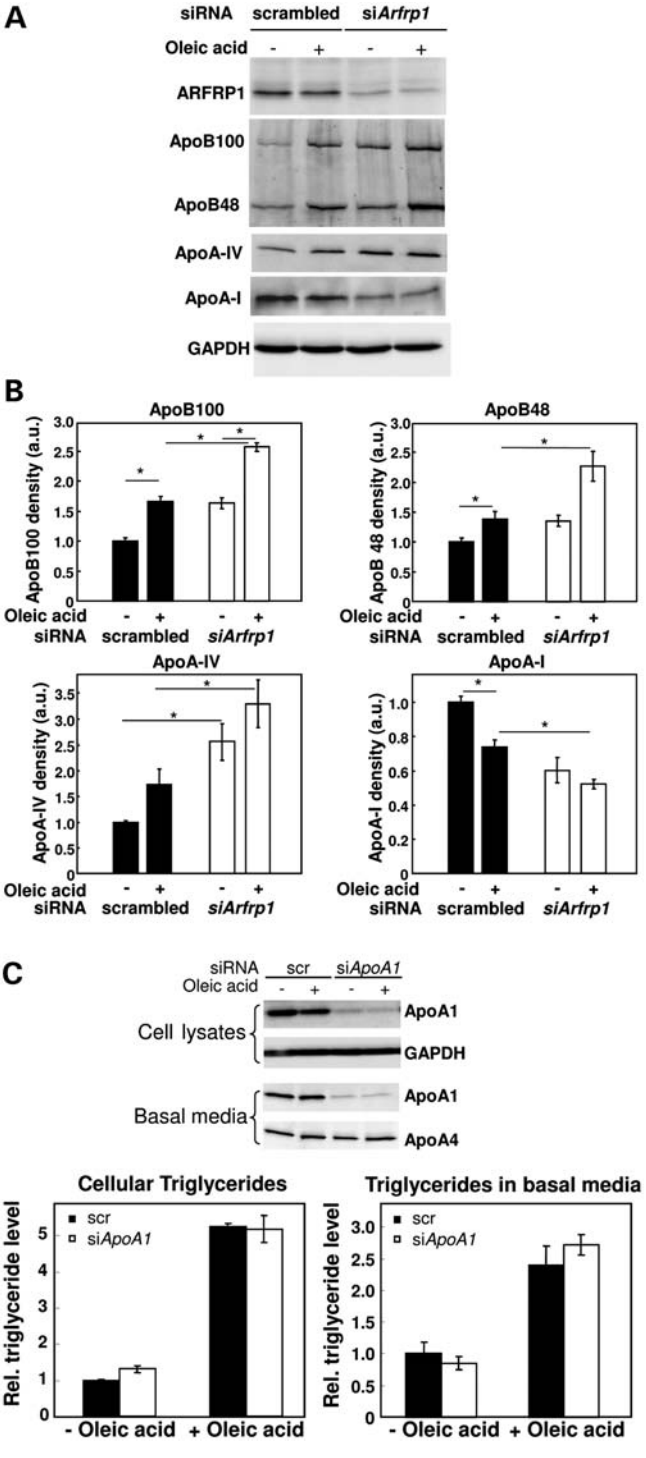

Figure 5. Reduced release of ApoA-I after the inhibition of *Arfrp1* expression by siRNA in Caco-2 cells. (**A**) Scrambled and *Arfrp1*-siRNA transfected cells were treated with or without oleic acid for 24 h and indicated proteins detected in the basolateral medium or cell lysate by western blotting. (**B**) Quantification of levels of indicated Apo released into the basolateral medium of control (scrambled) and *Arfrp1* knockdown (si*Arfrp1*) Caco-2 cells ($n = 8$). (**C**) Normal lipid release from Caco-2 cells after the down-regulation of *ApoA-I* expression. Caco-2 cells were transfected with scrambled or *ApoA1* siRNA and differentiated as described in Materials and methods. Cells were treated with 4 mM oleic acid for 24 h. The ApoA-I expression levels in the cell and in the basal media were determined by western blotting (top panel). Triacylglycerol levels were determined in the cells (bottom left panel) and the basal media (bottom right panel). Values represent the mean ± SEM.

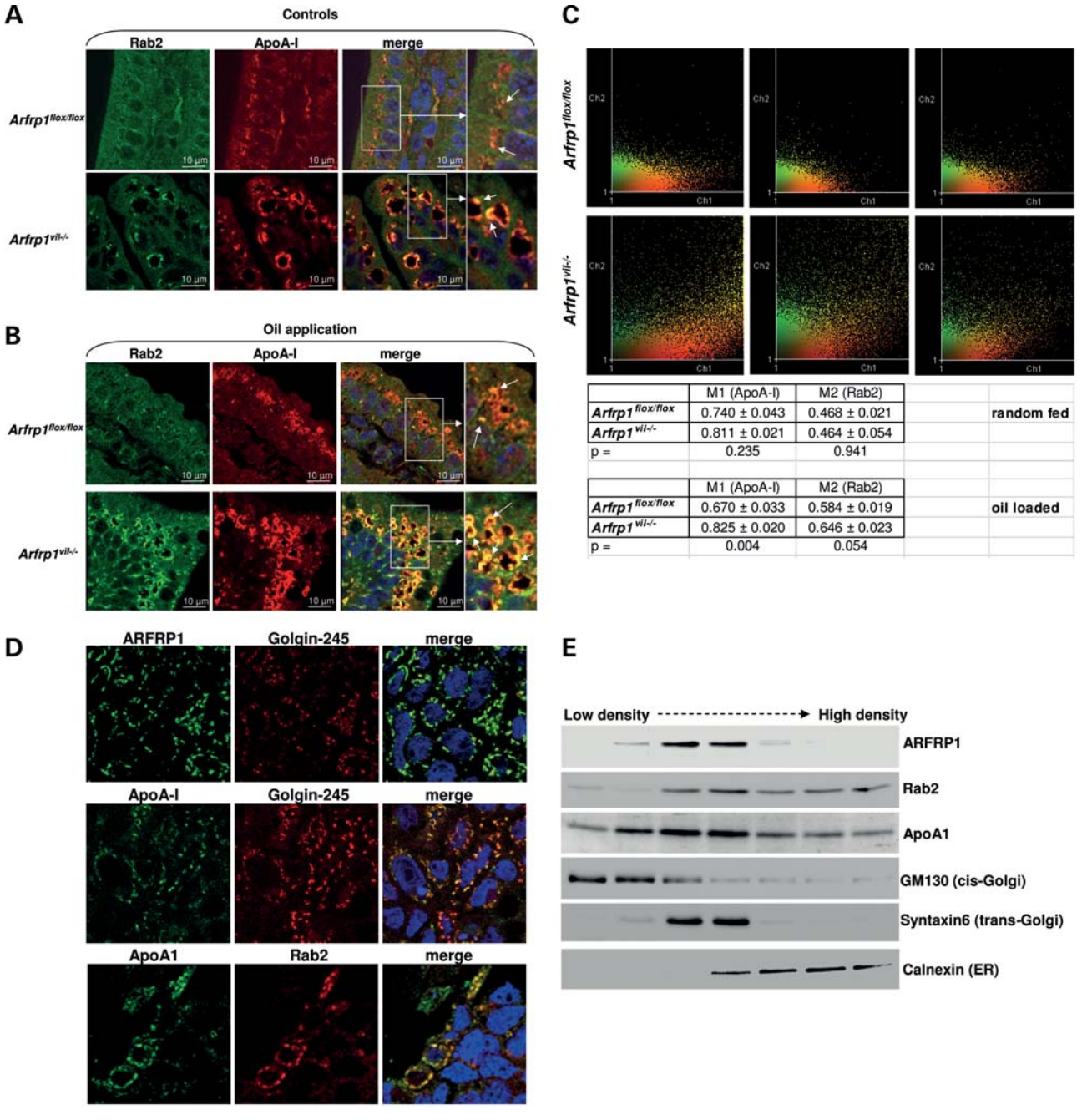

Figure 6. Co-localization of Rab2 with ApoA-I and its accumulation at Golgi membranes of intestinal *Arfrp1*$^{vil-/-}$ cells. (**A** and **B**) Immunohistochemical detection of Rab2 (left panels), ApoA-I (middle panels) and the merged picture (right panels) in sections of the small intestine of 4-week-old *Arfrp1*$^{flox/flox}$ and *Arfrp1*$^{vil-/-}$ mice that had free access to their diet (A) or which received an oil bolus after a 16-h fasting period (B). (**C**) Color scatter plots of pictures from intestinal epithelial sections of mice after the oil application (upper panel) and Mander's co-localization coefficient (lower panel) for channel 1 (M1; ApoA-I) and channel 2 (M2, Rab2). (**D**) Co-staining of ARFRP1 and Golgin-245 (upper panels), ApoA-I and Golgin-245 (middle panels) and Rab2 and ApoA-I (lower panels) in Caco-2 cells. (**E**) Co-localization of Rab2 with ApoA-1 and ARFRP1 in Golgi subcellular fractions. Subcellular fractions were isolated from differentiated Caco-2 cells with OptiPrep™ as described in Materials and methods. Indicated proteins in the fractions were concentrated and analyzed by western blotting.

membranes (7,9,10). Recently, Sinka *et al*. (13) discovered that GRIP domain Golgins also bind four members of the Rab family of small GTPases, Rab2, Rab6, Rab19 and Rab30. Thus, we tested the hypothesis that the deletion of *Arfrp1* results in an altered distribution of Rab proteins and that Rab proteins are co-localized with Apo.

Immunohistochemistry of Rab2 revealed a modified distribution in *Arfrp1*$^{vil-/-}$ cells when compared with *Arfrp1*$^{flox/flox}$ cells of fed mice (Fig. 6A, left panels); an effect which appeared more pronounced when mice had received an oil bolus (Fig. 6B, left panels). In control enterocytes, Rab2 was predominantly located in the cytosol and only partially

associated with membranes of the Golgi. In contrast, in *Arfrp1*$^{vil-/-}$ cells, Rab2 was mainly detected at large vesicular structures adjacent to the nuclei. Interestingly, co-staining of the sections with antibodies against Rab2 and ApoA-I indicated that Rab2 and ApoA-I are predominantly co-localized (Fig. 6A and B). The co-localization was most pronounced in intestinal sections of *Arfrp1*$^{vil-/-}$ mice, but also visible in the controls (see white arrows in higher magnifications; Fig. 6A and B). We quantified the level of co-localization of Rab2 and ApoA-I (Fig. 6C) by detecting the Mander's co-localization coefficient for channel 1 (M1; ApoA-I) and channel 2 (M2, Rab2). This analysis indicates that about two-thirds of ApoA-I is indeed co-located with Rab2. As shown in Figure 6C, we observed a significant increase in the co-localization of the two proteins in the *Arfrp1*$^{vil-/-}$ epithelium after the oil application.

In order to further test this hypothesis, we studied the subcellular localization of ARFRP1, Golgin-245, Rab2 and ApoA-I in Caco-2 cells. As expected, ARFRP1 and Golgin-245 were detected in the same compartment close to the nucleus, presumably the *trans*-Golgi (Fig. 6D, top panels). Furthermore, ApoA-I was co-localized with Golgin-245 (Fig. 6D, middle panels), and Rab2 with ApoA-I (Fig. 6D, bottom panels), supporting our conclusion that Rab2 may be involved in correct targeting of ApoA-I to chylomicrons in the Golgi apparatus. Similar results were obtained in subcellular fractions of Caco-2 cells. Western blot analysis of the subcellular fractions showed a co-localization of ARFRP1, Rab2 and ApoA-I in the *trans*-Golgi compartment, as indicated by the *trans*-Golgi marker Syntaxin6 (Fig. 6E). In order to test whether *Arfrp1* deletion affects the localization of COPII which together with Sar1 is essential for the transport of chylomicrons from the ER to the Golgi apparatus, we stained intestinal sections with an anti-COPII antibody. As shown in Supplementary Material, Figure S9, COPII is mainly located in the perinuclear region in control and *Arfrp1*$^{vil-/-}$ enterocytes without distinctive differences, suggesting the normal subcellular transport of pre-chylomicrons between ER and Golgi.

Furthermore, we tested this hypothesis by suppressing the expression of *Arl1, Golgin-245* and *Rab2* in Caco-2 cells and by detecting accumulation and release before and after the oil load. Similar to the effects observed after the suppression of *Arfrp1* (Fig. 2E), the cellular triglyceride content was significantly elevated, whereas the release at the basal site was markedly reduced after depleting the mRNA of *Arl1* (Fig. 7A), *Golgin-245* (Fig. 7B) or *Rab2* (Fig. 7C).

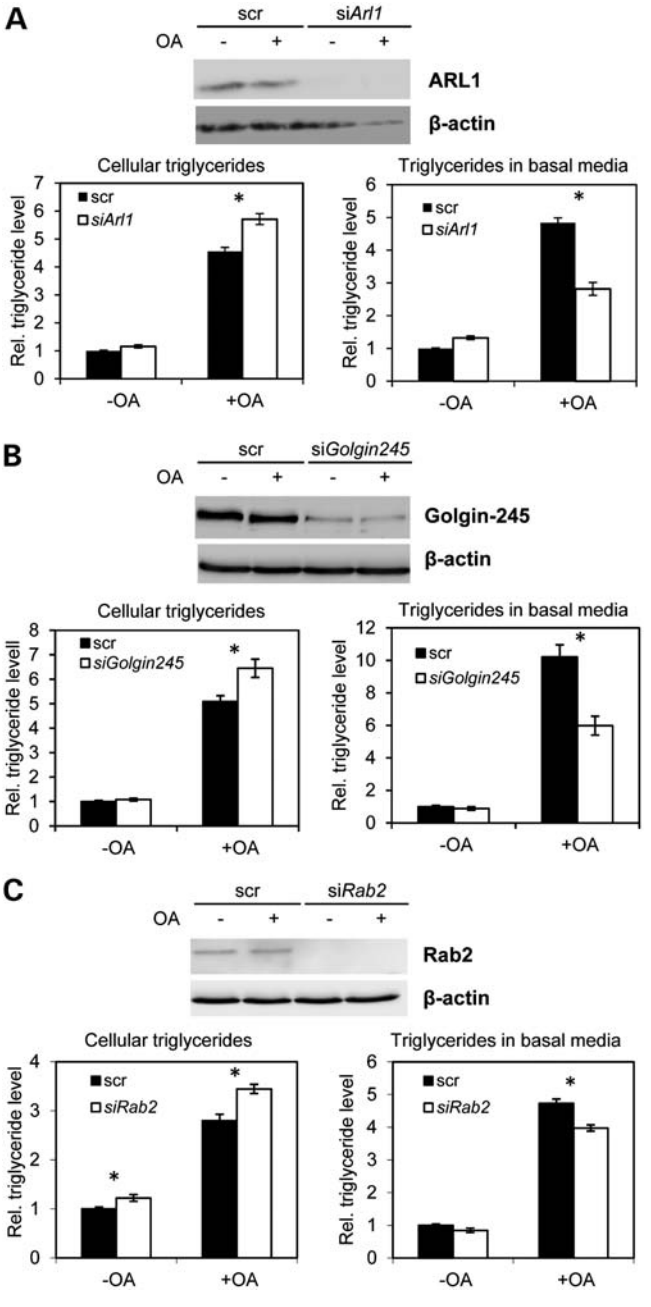

Figure 7. Impaired triglyceride release from Caco-2 cells after the suppression of *Arl1* (**A**), *Golgin-245* (**B**) and *Rab2* (**C**) expression. Caco-2 cells were transfected with scrambled or the indicated siRNAs and harvested 8 days after transfection for western blotting with the different antisera (top panels). Caco-2 cells were incubated with 4 mM oleic acid for 24 h, and triacylglycerol levels were measured in the cells (left panels) and the basal media (right panels).

DISCUSSION

In this work, we discovered the important role of the Golgi for the final lipidation of chylomicrons in the small intestine. We demonstrate that the *trans*-Golgi protein ARFRP1 plays an important role (i) for the lipidation of chylomicrons in the Golgi and (ii) the assembly of ApoA-I to the chylomicron. The intestine-specific *Arfrp1* null mutant mice showed reduced lipid absorption which resulted in the early postnatal growth retardation. Particularly, both *Arfrp1* intestine-specific knockout mice and *Arfrp1* depleted Caco-2 cells displayed changes in the composition of released Apo, indicating that ARFRP1 is involved in chylomicron maturation.

The assembly of chylomicrons starts in the ER where ApoB is translated and bound to the lipid core which is transferred by MTP to this compartment in order to generate the nascent lipoprotein particles (14–16). ApoA-IV is added to nascent particles in the ER to provide the surface stability of the particles (17). Subsequently, pre-chylomicrons bud off from the ER

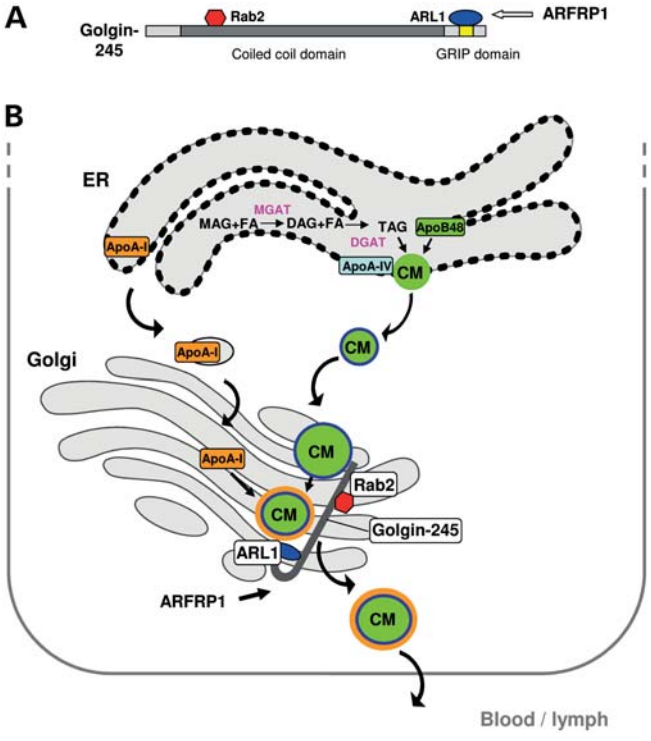

Figure 8. Model of the role of the ARFRP1-ARL1-Golgin-Rab2 cascade for chylomicron maturation. (**A**) ARFRP1 is necessary to recruit ARL1 to the Golgi, ARL1 binds to the GRIP domain of the scaffolding protein Golgin-245 which binds Rab2 via the coiled-coil domain. (**B**) Chylomicron formation in the ER and the Golgi. In the ER, monoacylglycerol acyltransferase (MGAT) and diacylglycerol acyltransferase (DGAT) catalyze the synthesis of triacylglycerol (TAG) which is incorporated into ApoB48-containing pre-chylomicrons. Subsequently, ApoA-IV binds to the pre-chylomicrons which are then released to the *cis*-Golgi and further lipidated in the Golgi. ApoA-I is synthesized in the ER and transported to the Golgi where it is attached to the chylomicrons. ApoA-I loaded chylomicrons are then transported through the Golgi, released on the *trans*-site and finally secreted into the lymph. We propose that the ARFRP1-ARL1-Golgin-Rab2 cascade is needed for an appropriate chylomicron assembly of ApoA-I, its transport through and lipidation within the Golgi.

membrane and translocate to the *cis*-Golgi. In the Golgi, pre-chylomicrons receive more lipids by MTP (18). All these steps appear not to be affected in *Arfrp1*$^{vil-/-}$ mice (see below). ApoA-I, which is released to a markedly reduced amount from *Arfrp1*$^{vil-/-}$ enterocytes (Figs 4 and 5), is also generated in the ER but transported to the Golgi separately from pre-chylomicron vesicles (Fig. 8) and added to the chylomicrons before the mature particle is secreted into the lymph (3,18).

Our data suggest that ARFRP1 plays a very specific role in the final lipidation of chylomicrons within the Golgi. We suggest that the first step of the pre-chylomicron maturation, the assembly of ApoB48 and lipid load in the ER, is not affected by the deletion of *Arfrp1*, because (i) ApoB48 is released (Fig. 4), (ii) MTP activity is not reduced (Supplementary Material, Fig. S8) and (iii) the localization of COPII, known to be required for the generation of PCTVs in the intestinal ER, is not altered in *Arfrp1*$^{vil-/-}$ mice (Supplementary Material, Fig. S9). However, we cannot prove certainly that the impact of *Arfrp1* deficiency on chylomicron biogenesis is a direct effect of Golgi (TGN) function or an indirect effect of downstream trafficking perturbations resulting from an altered Golgi. The fact that not only the depletion of *Arfrp1* but also that of three other proteins that are acting on the *trans*-site of the Golgi, ARL1, Golgin-245 and Rab2, results in impaired release of triglycerides (Fig. 7), supports our hypothesis that *Arfrp1* plays a specific role for the final lipidation of chylomicrons in the Golgi.

Our data indicate that the lipidation of chylomicrons in the Golgi and the assembly of ApoA-I to the chylomicron is impaired in *Arfrp1*$^{vil-/-}$ intestine, because the amounts of both triacylglycerol and ApoA-I were markedly reduced in the chylomicron fraction (Fig. 4C). This is supported by the fact that *Arfrp1* depleted Caco-2 cells released significantly less triacylglycerol (Fig. 2C–E) and ApoA-I (Fig. 5A and B). On the other hand, our data clearly demonstrate that the assembly of ApoA-I is not required for an appropriate lipidation of chylomicrons, because the suppression of ApoA-I expression in Caco-2 cells did not reduce the triacylglycerol release (Fig. 5C). We therefore conclude that the lipidation of chylomicrons in the Golgi occurs before ApoA-I is attached to these particles. It is described that MTP delivers the lipid core to ApoB not only in the ER but also—for further maturation of the particles—in the Golgi (18,19). Since we did not detect a reduced MTP activity in total lysates of Caco-2 cells in which *Arfrp1* expression was suppressed, we conclude that ARFRP1 does not modify MTP function.

ARFRP1 is located at the Golgi where it regulates the recruitment of ARL1 to Golgi membranes (7,9,10). We have recently shown that ARL1 is dislocated from the *trans*-Golgi to the cytosol in the intestinal epithelium of *Arfrp1*$^{vil-/-}$ mice (8). ARL1 itself binds GRIP domain proteins such as Golgin-245 and initiates their sorting to the Golgi (20). Recently, Sinka *et al*. (13) discovered an interaction of four Rabs with GRIP proteins, suggesting a connection between ARL and Rab protein pathways. Two Rab proteins, Rab2 (Fig. 6) and Rab6, exhibited altered distribution in epithelial cells of *Arfrp1*$^{vil-/-}$ mice and enhanced mRNA expression (data not shown). Rab2 is described to be involved in the regulation of the vesicle transport between the ER and the *cis*-Golgi. The expression of a constitutively active Rab2 mutant resulted in an impaired anterograde transport from the ER to the Golgi and an accumulation of vesicles in pre-Golgi membranes (21,22). We believe that as a consequence of the constant cytosolic localization of ARL1 in the *Arfrp1*$^{vil-/-}$ epithelial cells (8), Golgin-245 cannot be recruited to the *trans*-Golgi to facilitate the further transport of Rab2 vesicles through the Golgi (Fig. 7). However, up to now, we only can speculate that Rab2 associates with Golgin-245 or Golgin-97 in the intestinal epithelium because a direct interaction has not been shown so far. The finding that the knockdown of *Arl1* as well as that of *Rab2* resulted in a similar reduction in triglyceride release in Caco-2 cells (Fig. 7) supports our hypothesis but does not directly prove the direct connection of these proteins. Additional studies will be necessary to test whether Rab2 is physically associated with one of the golgin proteins.

In other words, the interaction between Rab2 and the ARL1-regulated scaffolding proteins Golgin-245 and Golgin-97 might be necessary for Rab2 to be released from the Golgi for further vesicular trafficking. Interestingly, Rab2 co-localized with ApoA-I which accumulated in

Arfrp1$^{vil-/-}$ cells and showed a marked reduction in its release in *Arfrp1*$^{vil-/-}$ mice (Fig. 4) and *Arfrp1* knockdown Caco-2 cells (Fig. 5). Furthermore, the fractionation of Caco-2 cells indicated that the major amount of Rab2 and ApoA-I are present in the *trans*-Golgi compartment (Fig. 6E). We therefore hypothesize that in enterocytes, the ARFRP1-ARL1-Golgin-Rab2 cascade is required for the final lipidation of chylomicrons and the transport of ApoA-I to the chylomicrons in the Golgi to complete the chylomicron maturation but that ARFRP1 acts independent and downstream of COPII and Sar1 (Fig. 8).

Several human diseases are characterized by defects in the synthesis and the secretion of the ApoB-containing lipoproteins. Familial hypobetalipoproteinemia is caused by mutations in the *APO-B* gene and is characterized by abnormally low plasma concentrations of ApoB and LDL cholesterol. Another syndrome with defective chylomicron formation, abetalipoproteinemia, is caused by mutations in the gene for MTP. This defect associates with very low plasma cholesterol and triacylglycerol levels, the absence of plasma ApoB and a lipid malabsorption syndrome (23). The third ApoB deficiency syndrome, Anderson's disease or chylomicron retention disease, is caused by mutations in the *SARA2* gene (protein Sar1b) (24–26). Sar proteins are members of the ARF family of GTPases like ARFRP1 and located at the ER (6), and their defects result in severe fat malabsorption (27). All chylomicron formation defects known so far are caused by alterations in the pre-chylomicron assembly. However, our data indicate that the trafficking and maturation of chylomicrons in the Golgi are also crucial steps for the normal lipid absorption as the defects in these steps affect lipid release from the mucosa and the whole-body lipid homeostasis.

The absorption of dietary fat is also of increasing concern because it participates in the rise of adiposity. Interestingly, intestinal chylomicron production is up-regulated in humans under conditions of insulin resistance. This chylomicron overproduction contributes to the highly prevalent dyslipidemia of insulin resistant patients (28). Therefore, our data significantly contribute toward the development of novel therapeutic strategies for treatments and the prevention of atherosclerosis and cardiovascular disease.

MATERIALS AND METHODS

Arfrp1$^{vil-/-}$ mice

The generation of intestine-specific *Arfrp1* null mutants was described before (8). In order to rescue the *Arfrp1*$^{vil-/-}$ mice, they were fed with carbohydrate-free high-fat diet (C1057 Sonderdiät; Altromin Spezialfutter, Lage, Germany) or a fat-depleted diet consisting of 26.5, 73.2 and 0.2% of calories from protein, carbohydrates and fat, respectively. All animal experiments were approved by the ethics committee of the Ministry of Agriculture, Nutrition, and Forestry (State of Brandenburg, Germany).

RNA preparation and first-strand cDNA synthesis

Total RNA from different tissues of the mice was extracted and cDNA synthesis was performed as described previously (29). The quality of cDNA was controlled by PCR with murine GAPDH primers (forward: 5′-ACC ACA GTC CAT GCC ATC AC-3′, reverse: 5′-TCC CAC CAC CCT GTT GCT GTA-3′).

Quantitative real-time PCR

Quantitative real-time PCR analysis was performed with the Applied Biosystems 7300 Real-time PCR System as described previously (29). Expression assays used for the determination of mRNA levels in jejunum are listed in Supplementary Material, Table S1. Data were normalized as described (29), whereas a β-actin expression assay was used as an endogenous control.

Body composition

For the examination of body fat and lean mass, a nuclear resonance spectrometer (Bruker-Mini-Spec-NMR-Analyzer mq10, Bruker Optics, Houston, USA) was used.

Plasma analysis

Blood glucose levels, plasma triglyceride and free fatty acid concentrations were determined as described (30).

Glucose tolerance test

Animals at the age of 5 weeks were fasted for 16 h prior to an oral application of glucose (20% solution, 2 g/kg body weight) and blood glucose concentrations were measured at 0, 7.5, 15, 30, 60 and 120 min from the tail tip.

Fat tolerance test

Five-week-old mice were fasted for 16 h and received 10 μl/g olive oil per gavage. Blood samples (30 μl) were collected via the tail vein prior to (basal, time 0) and 2, 3, 4, 6 and 12 h after the oral oil application for the determination of plasma triglyceride.

Detection of intestinal triglyceride secretion after the oil application and inhibition of lipoprotein lipase

Five-week-old mice were fasted for 5 h and received 10 μl/g olive oil per gavage. Twenty minutes later, Triton WR-1339 (15% in saline, 0.5 g/kg) was injected intravenously. About 30 μl blood samples were collected via the tail vein prior to and 30, 60 and 90 min after injection for the determination of plasma triglyceride concentrations. Mice were sacrificed and blood was collected by cardiac puncture, 100 min after Triton WR-1339 injection.

Oil-red O staining of intestinal sections

Cryosections of intestine of *Arfrp1*$^{flox/flox}$ and *Arfrp1*$^{vil-/-}$ animals were incubated with 0.3% oil-red O for 10 min, washed with 60% isopropanol and mounted in DAKO Faramount aqueous mounting medium.

Antibodies

We used the polyclonal antiserum against recombinant GST-ARFRP1 as described before (4,6). Commercial available antibodies used for western blotting and immunohistochemistry are listed in Supplementary Material, Table S2.

Immunohistochemistry

Paraffin sections of the small intestine of *Arfrp1*$^{flox/flox}$ and *Arfrp1*$^{vil-/-}$ animals at the age of 4 weeks were dewaxed in toluene and rehydrated. Antigen demasking was performed by heat treatment (microwave, 2.5 min, 850 W) in 10 mM Na-citrate, pH 6.0. Unspecific binding sites were blocked with the DAKO antibody diluent for 30 min. The indicated primary antibodies were applied overnight at 4°C in a humid chamber.

Subcellular distribution of SGLT1, Rab2, Rab6, ApoB48, ApoA-I and ApoA-IV was visualized by fluorescence-conjugated secondary antibodies. The sections were mounted in fluorescent mounting medium (Vectashield, Vector Labs, Burlingame, CA, USA) and analyzed with a Leica TCS SP2 Laser Scan inverted microscope. The intestinal tissues were sequentially scanned with an argon-krypton laser (488 nm) to excite the Alexa488 dye and with a helium-neon laser (543 nm) to excite the Alexa546 dye. The spectral detector recorded light emission at 510–560 and 580–660 nm, respectively. Images of 1024 × 1024 pixels were processed with Corel PHOTO-PAINT 10.0 (Coral Corporation).

Caco-2 cells and siRNA mediated suppression of *Arfrp1* expression

Caco-2 cells were cultured in DMEM containing high glucose, L-glutamine, 10% FBS and 1% penicillin–streptomycin. Transfection was performed as described. (31). Cells were transfected with 100 pmol/well scrambled or *Arfrp1* targeting siRNA using Lipofectamine 2000 (Invitrogen) in a 12-transwell system. Cells were maintained for 8 days on the transwell system with a medium change every 2 days. Caco-2 cells were oil-loaded with DMEM with 10% FBS and oleic acid:taurocholate complex (final concentration 4:0.5 mM) in the apical part for 24 h before harvest, while DMEM containing 0.1% FBS was supplied in the basal layer. On the culture day 8, cell layer and the basal medium were harvested for western blotting.

Detection of triglyceride on Caco-2 cells

Differentiated Caco-2 cells in a 6-transwell system were treated with 4 mM oleic acid for 24 h. Cells were harvested in 100 μl/well HB buffer and homogenized by needle-through with a 25G syringe, while lipids in the basal medium were extracted in chloroform–methanol (2:1, v/v), dried and resuspended in HB buffer. Triglyceride levels were estimated using Randox TR210 (Randox) according to the manufacturer's instruction.

Subcellular fraction of Caco-2 cells

Caco-2 cells maintained in a 6-transwell system were harvested in homogenization buffer [0.25 M sucrose, 1 mM EDTA, 20 mM HEPES KOH (pH7.4), protease inhibitor] and homogenized by needle-through with a 25G syringe. After removing the nuclei by centrifuging at 1500*g* for 10 min at 4°C, the homogenate was separated by Optiprep™ density gradient centrifugation according to the manufacturer's instruction (Axis-Shield, UK). The gradient was collected in 1 ml of fractions at the end of the centrifugation. Proteins in the fractions were concentrated using trichloroacetic acid (TCA) to be analyzed by western blotting.

MTP assay

Caco-2 cells were harvested and sonicated in homogenization buffer [10 mM Tris–HCl (pH 7.4), 150 mM NaCl, 1 mM EDTA, protease inhibitor]. The MTP assay was performed by incubating 100 μg of protein with 10 μl of donor solution and 10 μl of acceptor solution in total volume of 250 μl for 3 h at 37°C (Roar Biomedical, NY, USA). The fluorescence at 465 nm excitation and 538 nm emission wavelength was measured every 10 min. The results are expressed in arbitrary units corresponding to the fluorescence intensity transfer per minute.

Electron microscopy

Small intestine was fixed with 2.5% glutaraldehyde and 2% paraformaldehyde. Samples were rinsed in 0.1 M phosphate buffer and post-fixed with 1% osmiumtetroxide, dehydrated in ascending concentrations of methanol and propylenoxide and embedded into Epoxy resin. Blocks were trimmed, sectioned and viewed on the FEI EM 208 transmission electron microscope at ×13 000 magnification. Negatives were scanned at 800 dpi.

Western blot analysis

Scraped intestinal mucosa from *Arfrp1*$^{vil-/-}$ and *Arfrp1*$^{flox/flox}$ mice were homogenized and centrifuged for 1 h at 200 000*g* at 4°C. Membrane proteins (20 μg) were separated by SDS–PAGE and transferred onto nitrocellulose. For immunochemical detection, membranes were incubated with indicated primary antibodies and subsequently with secondary goat anti-rabbit IgG (H + L) peroxidase-conjugated antibody or rabbit anti-mouse IgG Fc-fragment peroxidase-conjugated antibody (1:20 000; Dianova, Hamburg, Germany).

Apos from Caco-2 cells were determined by western blotting of culture medium (ApoA-I and ApoA-IV, 35 μl; ApoB, TCA precipitation of 700 μl) and cell lysates (30 μg supernatant of an RIPA homogenate).

SUPPLEMENTARY MATERIAL

Supplementary Material is available at *HMG* online.

ACKNOWLEDGEMENTS

The skillful technical assistance of Michaela Rath, Monika Niehaus and Anett Seelig are gratefully acknowledged.

Conflict of Interest statement. None declared.

FUNDING

This work was supported by the Deutsche Forschungsgemeinschaft (Schu 750/5-3; GRK 1459; SFB 958) and by German Ministry of Education and Research (DZD: 01GI0922). B.C. is a fellow of the Alexander von Humboldt Foundation. Funding to pay the Open Access publication charges for this article was provided by German Ministry of Education and Research (DZD: 01GI0922).

REFERENCES

1. Minich, D.M., Vonk, R.J. and Verkade, H.J. (1997) Intestinal absorption of essential fatty acids under physiological and essential fatty acid-deficient conditions. *J. Lipid Res.*, **38**, 1709–1721.
2. Iqbal, J. and Hussain, M.M. (2009) Intestinal lipid absorption. *Am. J. Physiol. Endocrinol. Metab.*, **296**, E1183–E1194.
3. Mansbach, C.M. and Siddiqi, S.A. (2010) The biogenesis of chylomicrons. *Annu. Rev. Physiol.*, **72**, 315–333.
4. Schürmann, A., Massmann, S. and Joost, H.G. (1995) ARP is a plasma membrane-associated Ras-related GTPase with remote similarity to the family of ADP-ribosylation factors. *J. Biol. Chem.*, **270**, 30657–30663.
5. Kahn, R.A. (2003) ARF family GTPases. In *Proteins and Cell Regulation*. Kluwer Academic Publishers, Dordrecht, Boston, London, p. 1.
6. Kahn, R.A., Cherfils, J., Elias, M., Lovering, R.C., Munro, S. and Schürmann, A. (2006) Nomenclature for the human Arf family of GTP-binding proteins: ARF, ARL, and SAR proteins. *J. Cell Biol.*, **172**, 645–650.
7. Zahn, C., Hommel, A., Lu, L., Hong, W., Walther, D.J., Florian, S., Joost, H.G. and Schürmann, A. (2006) Knockout of Arfrp1 leads to disruption of ARF-like1 (ARL1) targeting to the trans-Golgi in mouse embryos and HeLa cells. *Mol. Membr. Biol.*, **23**, 475–485.
8. Zahn, C., Jaschke, A., Weiske, J., Hommel, A., Hesse, D., Augustin, R., Lu, L., Hong, W., Florian, S., Scheepers, A. *et al.* (2008) ADP-ribosylation factor-like GTPase ARFRP1 is required for trans-Golgi to plasma membrane trafficking of E-cadherin. *J. Biol. Chem.*, **283**, 27179–27188.
9. Panic, B., Whyte, J.R. and Munro, S. (2003) The ARF-like GTPases Arl1p and Arl3p act in a pathway that interacts with vesicle-tethering factors at the Golgi apparatus. *Curr. Biol.*, **13**, 405–410.
10. Setty, S.R., Shin, M.E., Yoshino, A., Marks, M.S. and Burd, C.G. (2003) Golgi recruitment of GRIP domain proteins by Arf-like GTPase 1 is regulated by Arf-like GTPase 3. *Curr. Biol.*, **13**, 401–404.
11. Hommel, A., Hesse, D., Völker, W., Jaschke, A., Moser, M., Engel, T., Blüher, M., Zahn, C., Chadt, A., Ruschke, K. *et al.* (2010) The ARF-like GTPase ARFRP1 is essential for lipid droplet growth and is involved in the regulation of lipolysis. *Mol. Cell. Biol.*, **30**, 1231–1242.
12. Van Greevenbroek, M.M.J. and de Bruin, T.W.A. (1998) Chylomicron synthesis by intestinal cells in vitro and in vivo. *Atherosclerosis*, **141**, S9–S16.
13. Sinka, R., Gillingham, A.K., Kondylis, V. and Munro, S. (2008) Golgi coiled-coil proteins contain multiple binding sites for Rab family G proteins. *J. Cell Biol.*, **183**, 607–615.
14. Kumar, N.S. and Mansbach, C.M. 2nd (1999) Prechylomicron transport vesicle: isolation and partial characterization. *Am. J. Physiol.*, **276**, G378–G386.
15. Gordon, D.A. and Jamil, H. (2000) Progress towards understanding the role of microsomal triglyceride transfer protein in apolipoprotein-B lipoprotein assembly. *Biochim. Biophys. Acta*, **1486**, 72–83.
16. Hussain, M.M., Shi, J. and Dreizen, P. (2002) Microsomal triglyceride transfer protein and its role in apoB-lipoprotein assembly. *J. Lipid Res.*, **44**, 22–32.
17. Lu, S., Yao, Y., Cheng, X., Mitchell, S., Leng, S., Meng, S., Gallagher, J.W., Shelness, G.S., Morris, G.S., Mahan, J. *et al.* (2006) Overexpression of apolipoprotein A-IV enhances lipid secretion in IPEC-1 cells by increasing chylomicron size. *J. Biol. Chem.*, **281**, 3473–3483.
18. Levy, E., Stan, S., Delvin, E., Menard, D., Shoulders, C., Garofalo, C., Slight, I., Seidman, E., Mayer, G. and And Bendayan, M. (2002) Localization of microsomal triglyceride transfer protein in the Golgi: possible role in the assembly of chylomicrons. *J. Biol. Chem.*, **277**, 16470–16477.
19. Siddiqi, S.A., Gorelick, F.S., Mahan, J.T. and Mansbach, C.M. II (2003) COPII proteins are required for Golgi fusion but not for endoplasmic reticulum budding of the pre-chylomicron transport vesicle. *J. Cell Sci.*, **116**, 415–427.
20. Lu, L. and Hong, W. (2003) Interaction of Arl1-GTP with GRIP domains recruits autoantigens Golgin-97 and Golgin-245/p230 onto the Golgi. *Mol. Biol. Cell*, **14**, 3767–3781.
21. Buffa, L., Fuchs, E., Pietropaolo, M., Barr, F. and Solimena, M. (2008) ICA69 is a novel Rab2 effector regulating ER-Golgi trafficking in insulinoma cells. *Eur. J. Cell Biol.*, **87**, 197–209.
22. Tisdale, E.J., Bourne, J.R., Khosravi-Far, R., Der, C.J. and Balch, W.E. (1992) GTP-binding mutants of rab1 and rab2 are potent inhibitors of vesicular transport from the endoplasmic reticulum to the Golgi complex. *J. Cell Biol.*, **119**, 749–761.
23. Gordon, D.A. (1997) Recent advances in elucidating the role of the microsomal triglyceride transfer protein in apolipoprotein B lipoprotein assembly. *Curr. Opin. Lipid*, **8**, 131–137.
24. Charcosset, M., Sassolas, A., Peretti, N., Roy, C.C., Deslandres, C., Sinnett, D., Levy, E. and Lachaux, A. (2008) Anderson or chylomicron retention disease, molecular impact of five mutations in the SAR1B gene on the structure and the functionality of Sar1b protein. *Mol. Genet. Metab.*, **93**, 74–84.
25. Silvain, M., Bligny, D., Aparicio, T., Laforêt, P., Grodet, A., Peretti, N., Ménard, D., Djouadi, F., Jardel, C., Bégué, J.M. *et al.* (2008) Anderson's disease (chylomicron retention disease): a new mutation in the SARA2 gene associated with muscular and cardiac abnormalities. *Clin. Genet.*, **74**, 546–552.
26. Cefalù, A.B., Calvo, P.L., Noto, D., Baldi, M., Valenti, V., Lerro, P., Tramuto, F., Lezo, A., Morra, I., Cenacchi, G. *et al.* (2010) Variable phenotypic expression of chylomicron retention disease in a kindred carrying a mutation of the Sara2 gene. *Metabolism*, **59**, 463–467.
27. Jones, B., Jones, E.L., Bonney, S.A., Patel, H.N., Mensenkamp, A.R., Eichenbaum-Voline, S., Rudling, M., Myrdal, U., Annesi, G., Naik, S. *et al.* (2003) Mutations in a Sar1 GTPase of COPII vesicle are associated with lipid absorption disorders. *Nat. Genet.*, **34**, 29–31.
28. Xiao, C. and Lewis, G.F. (2012) Regulation of chylomicron production in humans. *Biochim. Biophys. Acta*, **1821**, 736–746.
29. Buchmann, J., Meyer, C., Neschen, S., Augustin, R., Schmolz, K., Kluge, R., Al-Hasani, H., Jurgens, H., Eulenberg, K., Wehr, R. *et al.* (2007) Ablation of the cholesterol transporter adenosine triphosphate-binding cassette transporter G1 reduces adipose cell size and protects against diet-induced obesity. *Endocrinology*, **148**, 1561–1573.
30. Hesse, D., Hommel, A., Jaschke, A., Moser, M., Bernhardt, U., Zahn, C., Kluge, R., Wittschen, P., Gruber, A.D., Al-Hasani, H. *et al.* (2010) Altered GLUT4 trafficking in adipocytes in the absence of the GTPase Arfrp1. *Biochem. Biophys. Res. Commun.*, **394**, 896–903.
31. Zhang, M., Guller, S. and Huang, Y. (2007) Method to enhance transfection efficiency of cell lines and placental fibroblasts. *Placenta*, **28**, 779–782.